LETTER

doi:10.1038/nature16072

Liquids with permanent porosity

Nicola Giri[1], Mario G. Del Pópolo[2,3], Gavin Melaugh[2], Rebecca L. Greenaway[4], Klaus Rätzke[5], Tönjes Koschine[5], Laure Pison[6], Margarida F. Costa Gomes[6], Andrew I. Cooper[4] & Stuart L. James[1]

Porous solids such as zeolites[1] and metal–organic frameworks[2,3] are useful in molecular separation and in catalysis, but their solid nature can impose limitations. For example, liquid solvents, rather than porous solids, are the most mature technology for post-combustion capture of carbon dioxide because liquid circulation systems are more easily retrofitted to existing plants. Solid porous adsorbents offer major benefits, such as lower energy penalties in adsorption–desorption cycles[4], but they are difficult to implement in conventional flow processes. Materials that combine the properties of fluidity and permanent porosity could therefore offer technological advantages, but permanent porosity is not associated with conventional liquids[5]. Here we report free-flowing liquids whose bulk properties are determined by their permanent porosity. To achieve this, we designed cage molecules[6,7] that provide a well-defined pore space and that are highly soluble in solvents whose molecules are too large to enter the pores. The concentration of unoccupied cages can thus be around 500 times greater than in other molecular solutions that contain cavities[8–10], resulting in a marked change in bulk properties, such as an eightfold increase in the solubility of methane gas. Our results provide the basis for development of a new class of functional porous materials for chemical processes, and we present a one-step, multigram scale-up route for highly soluble 'scrambled' porous cages prepared from a mixture of commercially available reagents. The unifying design principle for these materials is the avoidance of functional groups that can penetrate into the molecular cage cavities.

The structural rigidity and robustness of solids allows them to contain permanent, uniform cavities of precise size and shape. By contrast, liquids have fluid structures, and any 'porosity' is limited to poorly defined and transient intermolecular cavities[11], most of which are smaller than typical molecules. The scaled particle theory[12,13] predicts that the solubility of a solute in a liquid is primarily influenced by the work required to generate the cavities that accommodate the solute. Thus, if high concentrations of permanent, molecule-sized cavities could be created in a liquid, the solvating and solute-transporting characteristics of that liquid should be strongly affected[5,14,15]. For example, solutes might become much more soluble because no work would be required to create cavities[12,13]. This effect should be specific to solute molecules of complementary size and shape to the pores, as is common for selective adsorption in porous solids.

We have prepared 'porous liquids' by taking rigid organic cage molecules, each of which defines a molecular pore space, and dissolving them at high concentration in a solvent that is too large to enter the pores (Fig. 1). Hence, the pores in the cages remain empty and available to solutes. In our first system, a crown ether, 15-crown-5, was chosen as the solvent because it is a liquid at room temperature and because it consists of large molecules with low surface curvature. Hence, no part of any solvent molecule can fit into the cage pores. Into this solvent were dissolved rigid organic cages. Each cage has a cavity of ~5 Å diameter at its centre that is accessible through four access windows of ~4 Å in diameter. Structurally similar but much less soluble cages are known to absorb small gas molecules into their pores in the solid state[6,7]. To achieve high solubility in the bulky 15-crown-5 solvent, each cage was functionalized on the outside with six crown ether groups by using a crown-ether functionalized diamine to prepare the cage. As a result, we could prepare, at room temperature, an extremely concentrated liquid phase (44 wt%) where just 12 solvent molecules are needed to dissolve each cage molecule. More typical solutions of molecules with cavities contain many hundreds or thousands of solvent molecules for each cavity. This liquid flows at room temperature, despite the high concentration of cages. The viscosity of the liquid was 20 cP to >140 cP in the range 298 K to 323 K, depending on the cage concentration (Supplementary Figs 10 and 11). In contrast, the viscosity of pure 15-crown-5 is 8.9 cP to 22.4 cP over this temperature range. Organic cages on their own can also form liquid phases close to room temperature if they have long alkyl chain substituents, but in those cases the chains occupy the cage cavities, thus removing the porosity[15].

Molecular dynamics (MD) simulations gave detailed insight into the structure of this 'porous liquid'. During 100-ns simulations, 100% of the cages remained empty at all times, both at 350 K and 400 K. Further modelling confirmed that occupation of the cages by the 15-crown-5 solvent molecules, or by the crown-ether substituents on the outside of the cages, would incur high free energy costs (full details are given in Supplementary Information). In fact, the free energy computed along a reaction coordinate that eventually forces the occupation of the cage by a 15-crown-5 solvent molecule shows no minimum when the solvent is inside the cage (Supplementary Fig. 14). Therefore, we conclude that the cages remain empty in the porous liquid over timescales longer than the MD simulations.

The distribution of cavity sizes, $\rho(R)$, was computed for the porous liquid, $\rho_{mix}(R)$, and for the pure 15-crown-5 solvent, $\rho_{sol}(R)$, both at the same temperature and pressure. Here $\rho(R)$ is the so-called insertion probability, which measures the likelihood that a hard sphere of radius R could be inserted at any arbitrary point within the liquid without overlapping with the van der Waals volume of any atom of the liquid[11]. The snapshot in Fig. 2a represents a typical configuration in the MD simulation for the 1:12 mixture at 350 K. The coloured surfaces show the empty cavities both inside (red) and outside (yellow) the cage cores that are accessible to spherical probes of radius 2.0–2.6 Å. This probe radius range was chosen because it reveals the cavities that are sufficiently large to accommodate methane as a solute molecule. Figure 2a shows that the cage cavities account for most of the large, methane-sized cavities in the liquid. This can be quantified with respect to the pure 15-crown-5 solvent by calculating the relative porosity of the mixture, defined as $V_{rel}(R) = \rho_{mix}(R)/\rho_{sol}(R)$. A value of $V_{rel}(R)$ greater than one indicates that the fractional free volume accessible to a spherical probe of radius R is larger in the porous liquid than in the pure solvent. As might be expected, the cages have no effect on the concentration of small, submolecular cavities in the liquid, and $V_{rel}(R)$ is around 1 for $R < 0.1$ nm (Fig. 2b). However, the

[1]School of Chemistry and Chemical Engineering, Queen's University Belfast, David Keir Building, Stranmillis Road, Belfast BT9 5AG, UK. [2]School of Mathematics and Physics, Queen's University Belfast, University Road, Belfast BT7 1NN, UK. [3]CONICET and Facultad de Ciencias Exactas y Naturales, Universidad Nacional de Cuyo, Padre Jorge Contreras 1300, CP5500 Mendoza, Argentina. [4]University of Liverpool, Department of Chemistry and Centre for Materials Discovery, Crown Street, Liverpool L69 7ZD, UK. [5]Technische Fakultät der Universität Kiel, Kaiserstrasse 2, D-24143 Kiel, Germany. [6]Institut de Chimie de Clermont-Ferrand, UMR 6296, CNRS, Université Blaise Pascal, 24 avenue Blaise Pascal, 63178 Aubière, France.

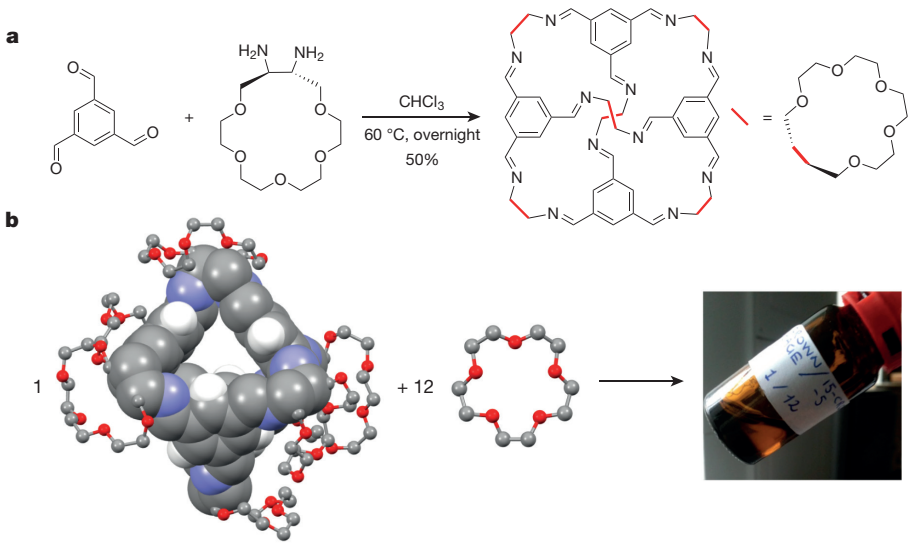

Figure 1 | Preparation of the porous liquid. a, Synthesis of the crown-ether cage. **b**, The empty, highly soluble cage molecule, left, defines the pore space; the 15-crown-5 solvent, middle, provides fluidity but cannot enter the cage cavities. The concentrated solution (porous liquid) flows at room temperature, right. Key: C, grey; O, red; N, blue; H, white. Space-filling rendering highlights the core of the cage. Ball and stick rendering represents the crown-ether substituents on the cage and the 15-crown-5 solvent. All H atoms except those attached to aromatic rings of the cage compound have been omitted for clarity.

cages dramatically increase the concentration of cavities with radii in the range 0.1–0.25 nm. This effect is particularly strong at 350 K, where $V_{rel}(R)$ approaches 1,900 for $R = 0.24$ nm. $V_{rel}(R)$ is larger at 350 K than at 400 K because more large cavities form transiently in the solvent at higher temperatures owing to increased thermal motion. Overall, the fractional void volume in the porous liquid due to the cages was estimated as 0.7% of the total volume. This is small compared to typical pore volumes in porous solids, but it can dramatically affect the solubility of solutes in the liquid.

Positron (e^+) annihilation lifetime spectroscopy (PALS) experiments were used to investigate whether the cages in the porous liquid were empty. PALS probes the electron density distribution in materials, in particular the presence of empty pores. Exposure of an insulating material to a positron source such as ^{22}Na leads to the formation of ortho-positronium (o-Ps; that is, an e^+ and an e^- with parallel spins bound into an exotic atom) within the material. The lifetime of the positron (that is, the time between injection of the positron into the material and the decay of o-Ps) can be correlated to the average pore diameter in the material by a well-established model[16], that is, the larger the pore the lower the decay probability and the longer the lifetime. Thus, by comparing the o-Ps lifetimes observed in the pure (solid) cage material, the pure 15-crown-5 solvent and the porous liquid, we investigated whether the cages in the porous liquid were empty. Several measurements were made on each material to check for reproducibility and to enable separation of the raw data for the porous liquid into constituent components. The o-Ps lifetime of 2.05 ± 0.1 ns measured for the pure solid cage at 30 °C correlates to an average cavity diameter of 0.55 nm, in reasonable agreement with our MD simulations. The o-Ps lifetime of 3.00 ± 0.1 ns for the pure 15-crown-5 solvent at 30 °C is also in agreement with previous literature[17]. This latter measurement can be explained by the known phenomenon of o-Ps bubble formation[17], rather than by any pre-existing pores in the pure 15-crown-5 solvent. The o-Ps lifetime measured for the porous liquid at 30 °C was 2.34 ± 0.02 ns. If the cages are empty in the porous liquid, then the o-Ps lifetime should correspond to a combination of the lifetimes measured for the pure cage and the pure 15-crown-5 solvent.

To investigate whether the o-Ps lifetime for the porous liquid could be separated into these individual contributions, both free and forced fits were applied to the raw data. Allowing both components to refine freely did not give a satisfactorily clear separation (large error bars were

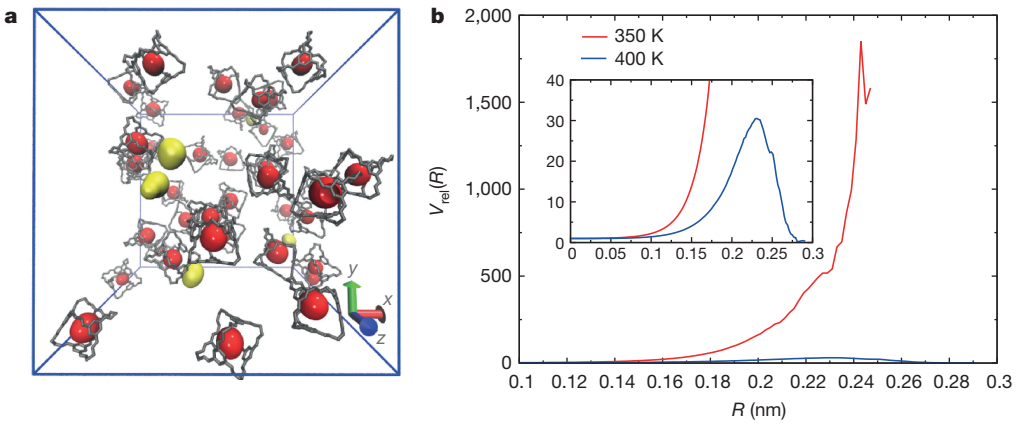

Figure 2 | Molecular simulations for the porous liquid show unoccupied molecular-sized pores. a, Representative configuration of the porous liquid at 350 K. To highlight the cage cores, crown-ether solvent molecules and crown-ether substituents on the cages have been omitted. Red and yellow surfaces indicate empty pores inside or outside the cages, respectively. **b**, Relative porosity, $V_{rel}(R)$, of the porous liquid at 350 K and 400 K. Inset, expansion of the 400 K result. At 350 K, the porous liquid has around 1,900 times as many methane-sized cavities (probe radius ~0.24 nm) than does the pure solvent.

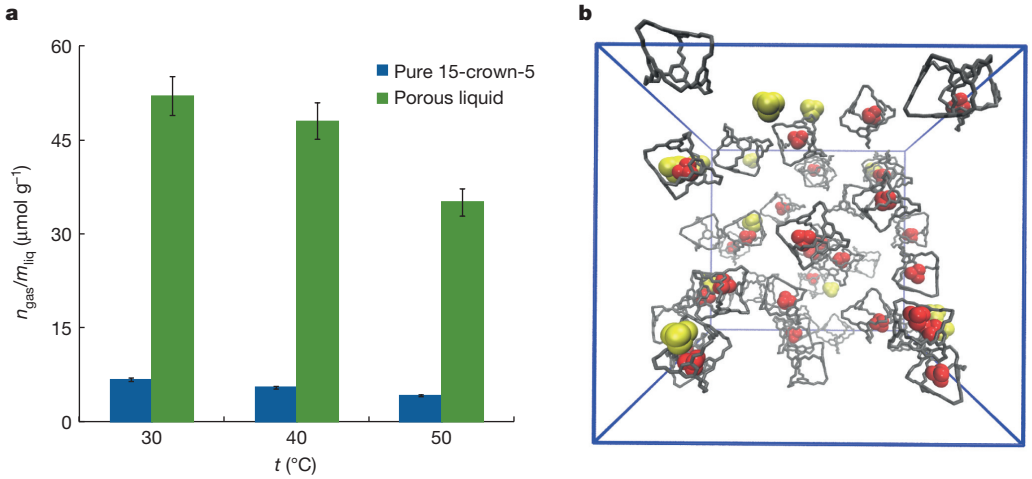

Figure 3 | Dissolution of methane in the porous liquid. a, Methane is around 8 times more soluble per mass of the porous liquid at 1 atm pressure than per mass of the pure 15-crown-5 solvent. Error bars represent overall uncertainty of experimental data calculated by error propagation of the s.d. of the measured quantities. **b**, Molecular simulation of the porous liquid with dissolved methane (grand canonical Monte Carlo simulation at 350 K, 1 atm). Methane is shown in red when inside a cage core (<2.5 Å from the cage centre) or yellow when outside. Solvent and cage substituents are omitted for clarity.

observed; see Supplementary Fig. 23). However, a forced fit where one component was fixed at 3.00 ns, consistent with the anticipated contribution from the pure 15-crown-5 solvent, and where the other component was allowed to refine freely, did result in satisfactory separation of these two components (Supplementary Fig. 24). The freely refined component had a value of 1.91 ± 0.08 ns, which corresponds well to the lifetime observed for the pure empty cage (2.05 ± 0.1 ns). The PALS measurements are thus consistent with the presence of empty cages, or molecular 'pores', in the porous liquid.

Both MD simulations and PALS data suggested that the porous liquid might have a dramatically increased capacity to dissolve solute molecules up to ~0.5 nm in diameter relative to the pure crown solvent, particularly at temperatures of 350 K or lower (Fig. 2b). Acidic gases, such as carbon dioxide, are absorbed readily by conventional, non-porous solvents such as water or aqueous amines[4]. We therefore focused our initial studies on methane, the main component of natural gas. Methane, like other important gases such as hydrogen, lacks the Lewis acidity of carbon dioxide and hence cannot be absorbed using liquid amines. The methane solubility in pure 15-crown-5 at 30 °C was found to be 6.7 μmol g^{-1}. By contrast, the solubility of methane in the porous liquid was 52 μmol g^{-1} at 30 °C. This represents, approximately, an eightfold increase in solubility in the porous liquid compared to the pure solvent. The methane solubility decreased at higher temperatures, both in the porous liquid and in the non-porous solvent, but the solubility was much higher in the porous liquid at all temperatures studied (Fig. 3a).

Molecular simulations for solutions of methane in the porous liquid suggested that most methane molecules would reside in the cage cavities, rather than in transient intermolecular cavities (see Fig. 3b and Supplementary Information for details). For example, at 350 K and a gas pressure of 1 atm, 70% of the methane molecules in the liquid were located inside the cages, that is, less than 2.5 Å from a cage centre. These simulations support the methane solubility measurements by predicting that methane should be significantly more soluble in the porous liquid. The enhanced solubility cannot be ascribed to a simple solvating effect of the aromatic cage walls because methane solubility in pure aromatic solvents, such as benzene, is lower than for the porous liquid (26.8 μmol g^{-1} at 25 °C)[18,19]. The methane absorption capacity is remarkably high for a liquid, albeit much lower than for many porous solids, such as zeolitic imidazolate frameworks[20].

This porous molecular liquid differs fundamentally from porous macromolecular liquids containing hollow colloidal silica spheres[21]. Solutions of other types of organic cages with smaller internal pores, known as carcerands and cryptophanes, also have pores that are most probably unsolvated because even relatively small solvent molecules are excluded[8–10]. The existence of permanent cavities in these carcerand/cryptophane systems was not, however, supported by simulations or by PALS measurements, nor was enhanced bulk solubility of gases noted. This is probably because the solutions were very dilute; for example, based on a 2 mM host solution of a cryptophane in $CDCl_3$, as described in ref. 10, the molar ratio of cage to solvent molecules was 1:6,000, compared with the 1:12 solution that we study here. The cryptophane cavity volume in that study[10] was reported to be 81 Å^3. If the cryptophane is assumed not to have collapsed, then this represents just 0.01% of the total volume, which is 70 times lower than in our study. The much higher density of cavities in our system demonstrates a previously unexplored way to control the bulk solubility of gases and other solutes in liquids.

Although porous liquids of the type we report here might not be competitive with porous solids for gas storage, we envisage other applications, such as gas separation, which utilize the high concentration of prefabricated cavities in the liquid. A practical scale-up issue is the six-step cage synthesis (Supplementary Information), which has modest overall yield (3.1%–6.5%). Also, the viscosity of the crown-ether porous liquid is rather high (20 cP to >140 cP). We therefore developed an alternative, more scalable route, where a mixture of diamines is used to make a mixture of 'scrambled' cages[22] that have the same core cage dimensions as the crown-ether derivative discussed above. The resulting mixture of scrambled cage molecules has much higher solubility in common organic solvents than similar cages prepared from a single diamine (see table, Fig. 4a) because of increased structural disorder[23].

Multi-gram quantities of the scrambled cage mixture are easily prepared from commercially available starting materials via this one-step synthesis (Fig. 4a; 77% yield). As for the crown-ether derivatized cage described above, this scrambled cage mixture can form concentrated solutions (>10 wt%) in a solvent, hexachloropropene (PCP), which like 15-crown-5 is size-excluded from the cage cavity. These solutions were at least ten times less viscous (11.7 cP at 295 K, 0.112 mmol of cage per 1 g of PCP) than the crown-ether-based porous liquid described above at comparable cage concentrations because of the lack of bulky crown-ether substituents. Like the porous liquid prepared from the crown-ether derivatized cage, this porous liquid prepared from the scrambled mixture of cages showed much higher methane gas solubility than the non-porous PCP solvent (51 μmol g^{-1} versus 6.7 μmol g^{-1} at 293 K). Other gases such as nitrogen, carbon dioxide and xenon also showed enhanced solubilities in the scrambled-cage-based porous liquid, and

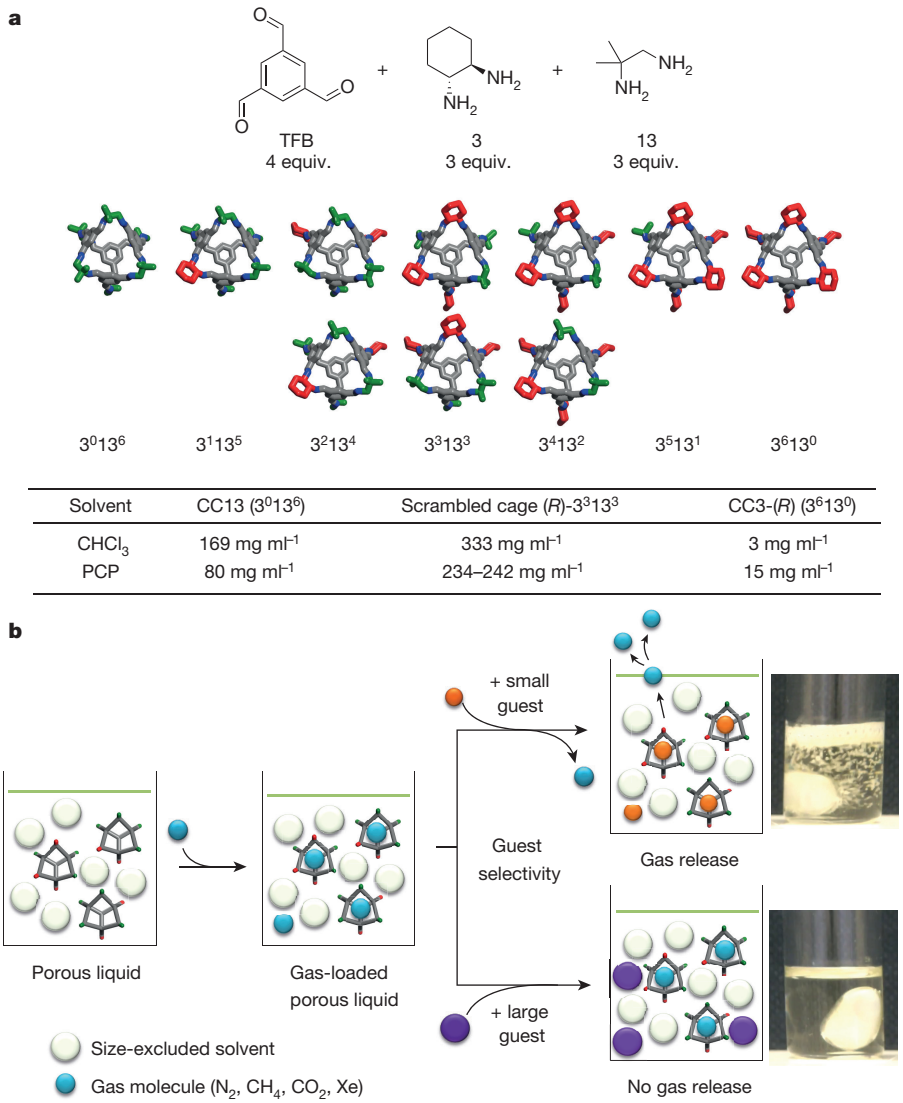

Solvent	CC13 ($3^0 13^6$)	Scrambled cage (*R*)-$3^3 13^3$	CC3-(*R*) ($3^6 13^0$)
$CHCl_3$	169 mg ml^{-1}	333 mg ml^{-1}	3 mg ml^{-1}
PCP	80 mg ml^{-1}	234–242 mg ml^{-1}	15 mg ml^{-1}

Figure 4 | Porous liquids based on scrambled cages. a, Reaction of the trialdehyde, TFB, with two different diamines, 3 and 13, bearing cyclohexane and dimethyl groups, respectively, gives rise to a statistical mixture of cages which differ from each other in the number and positions of their dimethyl (green) and cyclohexane (red) groups. Nomenclature $3^x 13^y$ defines the number of cyclohexane groups (x) and number of dimethyl groups (y) for each cage. Three cages ($3^2 13^4$, $3^3 13^3$ and $3^4 13^2$) each exist as a pair of isomers, as indicated by the additional structures shown in the second row of products. The average structure of this scrambled mixture is $3^3 13^3$. Mixtures of 'scrambled' cages were thus prepared in a scalable, one-pot synthesis and are up to 100 times more soluble than cages prepared from single diamines, such as CC3-(*R*) (ref. 6) or CC13 (ref. 23). PCP is hexachloropropene solvent which is size-excluded from the cage cavities. **b**, The porous liquids show enhanced solubilities for methane, nitrogen, carbon dioxide and xenon (Supplementary Figs 32–35). Addition of a small, interpenetrating guest, $CHCl_3$, liberates xenon gas rapidly from a xenon-saturated porous liquid (top photograph; Supplementary Video 1) whereas addition of a large, size-excluded guest, 1-*t*-butyl-3,5-dimethylbenzene, does not (bottom photograph).

the trend in gas solubility follows the calculated Henry's coefficients[24] and isosteric heats of sorption for these gases in solid porous cages of this size and geometry (Supplementary Fig. 35), again suggesting that gas solubility is dominated by the unoccupied cage cavities. A shift in the ^{1}H NMR signal for methane was observed from −0.24 p.p.m. (using tetramethylsilane, TMS, as standard) in neat PCP to −2.80 p.p.m. in the scrambled-cage-based porous liquid (Supplementary Fig. 30). This strong shielding effect ($\Delta\delta = -2.56$ p.p.m.) supports the presence of methane in the cage cavities of the scrambled porous liquid on the NMR timescale[9,10].

As for the porous liquids prepared from crown-ether derivatized cages, the increased gas solubility in the scrambled-cage-based porous liquid stems from the absence of functional groups that can penetrate the cage cavities, in this case because the peripheral methyl groups on the scrambled cages are too small to do this. By contrast, other organic molecules of the correct size can compete with gases for the cage cavities. For example, addition of chloroform rapidly displaces xenon from a sample of the scrambled-cage-based porous liquid that was saturated with xenon, whereas addition of a larger, size-excluded guest, 1-*t*-butyl-3,5-dimethylbenzene, does not (Fig. 4b; Supplementary Video 1). This allows dramatic solubility switching to occur with the addition of a remarkably small amount of a second, smaller solvent. For example, 10.05 ml STP of xenon is released from 5.74 g of the scrambled-cage-based porous liquid by addition of just 0.046 ml (1.29 vol.%) of $CHCl_3$. This remarkably sharp switching behaviour can be ascribed to a molecular displacement mechanism, rather than to a change in the bulk solvent properties.

Online Content Methods, along with any additional Extended Data display items and Source Data, are available in the online version of the paper; references unique to these sections appear only in the online paper.

Received 12 December 2014; accepted 12 October 2015.

1. Wright, P. A. *Microporous Framework Solids* (Royal Society of Chemistry, 2007).
2. Cheetham, A. K., Férey, G. & Loiseau, T. Open-framework inorganic materials. *Angew. Chem. Int. Edn* **38,** 3268–3292 (1999).
3. Kitagawa, S., Kitaura, R. & Noro, S. Functional porous coordination polymers. *Angew. Chem. Int. Edn* **43,** 2334–2375 (2004).
4. D'Alessandro, D. M., Smit, B. & Long, J. R. Carbon dioxide capture: prospects for new materials. *Angew. Chem. Int. Edn* **49,** 6058–6082 (2010).
5. O'Reilly, N., Giri, N. & James, S. L. Porous liquids. *Chem. Eur. J.* **13,** 3020–3025 (2007).
6. Tozawa, T. *et al.* Porous organic cages. *Nature Mater.* **8,** 973–978 (2009).
7. Jones, J. T. A. *et al.* Modular and predictable assembly of porous organic molecular crystals. *Nature* **474,** 367–371 (2011).
8. Robbins, T. A., Knobler, C. B., Bellew, D. R. & Cram, D. J. A highly adaptive and strongly binding hemicarcerand. *J. Am. Chem. Soc.* **116,** 111–122 (1994).
9. Chaffee, K. E., Fogarty, H. A., Brotin, T., Goodson, B. M. & Dutasta, J.-P. Encapsulation of small gas molecules by cryptophane-111 in organic solution. 1. Size- and shape-selective complexation of simple hydrocarbons. *J. Phys. Chem. A* **113,** 13675–13684 (2009).
10. Little, M. A. *et al.* Synthesis and methane-binding properties of disulfide-linked cryptophane-0.0.0. *Angew. Chem. Int. Edn* **51,** 764–766 (2012).
11. Pohorille, A. & Pratt, L. R. Cavities in molecular liquids and the theory of hydrophobic solubilities. *J. Am. Chem. Soc.* **112,** 5066–5074 (1990).
12. Pierotti, R. A. The solubility of gases in liquids. *J. Phys. Chem.* **67,** 1840–1845 (1963).
13. Pierotti, R. A. A scaled particle theory of aqueous and non-aqueous solutions. *Chem. Rev.* **76,** 717–726 (1976).
14. Giri, N. *et al.* Alkylated organic cages: from porous crystals to neat liquids. *Chem. Sci.* **3,** 2153–2157 (2012).
15. Melaugh, G., Giri, N., Davidson, C. E., James, S. L. & Del Pópolo, M. G. Designing and understanding permanent microporosity in liquids. *Phys. Chem. Chem. Phys.* **16,** 9422–9431 (2014).
16. Mogensen, O. E. (ed.) *Positron Annihilation in Chemistry* (Springer Series in Chemical Physics 58, Springer, 1995).
17. Mahmood, T., Cheng, K. L. & Yean, Y. C. Microanalysis of open spaces in crown ethers by using a novel probe: positron annihilation spectroscopy. In *Third International Workshop on Positron and Positronium Chemistry* (ed. Jean, Y. C.) 640 (World Scientific, 1990).
18. Lannung, A. & Gjaldbæk, J. C. The solubility of methane in hydrocarbons, alcohols, water and other solvents. *Acta Chem. Scand.* **14,** 1124–1128 (1960).
19. Darwish, N. A., Gasem, K. A. M. & Robinson, R. L. Jr. Solubility of methane in benzene, naphthalene, phenanthrene and pyrene at temperatures from 323 to 433 K and pressures to 11.3 MPa. *J. Chem. Eng. Data* **39,** 781–784 (1994).
20. Houndonougbo, Y. *et al.* A combined experimental–computational investigation of methane adsorption and selectivity in a series of isoreticular zeolitic imidazolate frameworks. *J. Phys. Chem. C* **117,** 10326–10335 (2013).
21. Zhang, J. *et al.* Porous liquids: a promising class of media for gas separation. *Angew. Chem. Int. Edn* **54,** 932–936 (2015).
22. Jiang, S. *et al.* Porous organic molecular solids by dynamic covalent scrambling. *Nature Commun.* **2,** 207 (2011).
23. Hasell, T. *et al.* Controlling the crystallization of porous organic cages: molecular analogs of isoreticular frameworks using shape-specific directing solvents. *J. Am. Chem. Soc.* **136,** 1438–1448 (2014).
24. Chen, L. *et al.* Separation of rare gases and chiral molecules by selective binding in porous organic cages. *Nature Mater.* **13,** 954–960 (2014).

Supplementary Information is available in the online version of the paper.

Acknowledgements This work was funded by the Leverhulme Trust (F/00 203/T) and by EPSRC (EP/C511794/1). M.G.D.P. acknowledges financial support from ANPCyT (PICT-2011-2128) and from the EC-H2020, MSCRISE-2014 programme, through project 643998 ENACT. L.P. and M.C.G. acknowledge support from the Contrat d'Objectifs Partagés (CNRS, Blaise Pascal University, and the Auvergne Regional Government, France). A.I.C. acknowledges the European Research Council under the European Union's Seventh Framework Programme/ERC Grant Agreement no. 321156 for financial support. We thank M. E. Briggs for assistance with the cage syntheses.

Author Contributions N.G. and R.L.G. synthesized the porous crown cage. M.D.P. and G.M. carried out the molecular simulations. K.R. and T.K. performed the PALS measurements. M.C.G. and L.P. measured the methane gas solubilities for the crown cage porous liquid. R.L.G. and A.I.C. conceived the synthesis of the scrambled porous imine cages. R.L.G synthesized and characterized the scrambled cage porous liquid and measured its gas solubilities. S.L.J. led the project overall and conceived the design of the porous liquid based on the crown-ether cage together with N.G. S.L.J. and A.I.C. led the writing of the manuscript with contributions from all co-authors.

Additional Information Reprints and permissions information is available at www.nature.com/reprints. The authors declare no competing financial interests. Readers are welcome to comment on the online version of the paper. Correspondence and requests for materials should be addressed to S.L.J. (S.James@qub.ac.uk).

METHODS

Synthesis of the porous crown-ether cage. The cage was prepared in six steps. The details for the five-step synthesis of the crown-ether diamine, (15*S*,16*S*)-1,4,7,10,13-pentaoxacycloheptadecane-15,16-diamine, are given in Supplementary Information. Reaction of this diamine (8 equiv.) with 1,3,5-triformylbenzene (4 equiv.) in chloroform at 60 °C gave the desired imine cage in a one-pot [4 + 6] cycloimination reaction (Fig. 1a)[6,7]. Melting point, decomposes >180 °C; IR (ν_{max} in cm^{-1}) 2,858, 1,649, 1,598, 1,445, 1,352, 1,298, 1,250, 1,111, 978, 943, 882; ^{1}H NMR (500 MHz, $CDCl_3$) δ_H (in p.p.m.) 8.12 (12 H, s), 7.92 (12 H, s), 4.03 (12 H, d, J = 7.0 Hz), 3.75–3.58 (120 H, m); ^{13}C NMR (126 MHz, $CDCl_3$) δ_C (in p.p.m.) 161.06, 136.56, 130.20, 73.25, 72.68, 71.70, 71.09, 70.87, 70.60; HRMS (ES+) calc. for $C_{108}H_{156}N_{12}Na_2O_{30}$ $[M + 2Na]^{2+}$ 1,073.5422, found 1,073.5496; CHN analysis calc. for $C_{108}H_{156}N_{12}O_{30}$: C, 61.70; H, 7.48; N, 7.99; found: C, 59.57; H, 7.34; N, 7.74.

Synthesis of scrambled porous cages. The scrambled cage mixture was synthesized in one step via the reaction of 1,3,5-triformylbenzene (4 equiv.), 1,2-diamino-2-methylpropane (ref. 23) (13, 3 equiv.) and (*R*,*R*)-1,2-diaminocyclohexane (ref. 6) (3, 3 equiv.) in dichloromethane at room temperature (yield, 77%). Full details are given in Supplementary Information.

Preparation of the porous liquids. The crown cage (0.100 g, 0.0475 mmol, 1 equiv.) was dissolved in 15-crown-5 (113 µl, 0.5707 mmol, 12 equiv.) by sonicating the mixture for 2 h, resulting in a viscous, pale yellow liquid. For the scrambled cages, the solid material was first degassed and then dissolved in rigorously purified hexachloropropene (PCP) to form a pale yellow 10 wt% solution.

Molecular dynamics (MD) simulations. Atomistic models for the crown cage were constructed using the OPLS all atom force-field[25]. We computed the free energy cost for introducing a single 15-crown-5 molecule into a cage cavity using the umbrella sampling (US) method[26] combined with the weighted histogram analysis method (WHAM)[27]. The US simulations were performed with the GROMACS-4.5.3 code[28], in the canonical ensemble (NVT) at 400 K, using a timestep of 0.001 ps. Bulk MD simulations were run on a sample consisting of 40 cages and 480 solvent molecules enclosed in a cubic and periodic simulation box in the isobaric-isothermal ensemble (NPT), using a timestep of 1 fs, a Nosé–Hoover thermostat[29,30], and a Parrinello–Rahman barostat[31], with time constants of 0.1 ps and 1 ps, respectively. Lennard–Jones interactions were cut off at 1.4 nm, while Coulomb forces were computed using the smooth particle mesh Ewald technique[32]. Full computational details are given in Supplementary Information.

Positron annihilation lifetime spectroscopy (PALS). Measurements were performed as a function of temperature in a standard experimental set-up, as described previously[33].

Gas solubility measurements. An isochoric technique[34] was used to measure methane gas solubility in the pure 15-crown-5 solvent and in the porous liquid. For the scrambled cages, gas solubilities were either measured by ^{1}H NMR (for example, for methane) or, for larger bulk samples of the porous liquid, by displacing the gas by addition of one molar equivalent (relative to the cage) of a second, small guest (for example, chloroform, Fig. 4b) and measuring the amount of gas (for example, xenon) evolved.

25. Jorgensen, W. L., Maxwell, D. S. & Tirado-Rives, J. Development and testing of the OPLS all-atom force field on conformational energetics and properties of organic liquids. *J. Am. Chem. Soc.* **118,** 11225 (1996).
26. Roux, B. The calculation of the potential of mean force using computer simulations. *Comput. Phys. Commun.* **91,** 275 (1995).
27. Kumar, S., Rosenberg, J. M., Bouzida, D., Swendsen,R. H. & Kollman, P. A. Multidimensional free-energy calculations using the weighted histogram analysis method. *J. Comput. Chem.* **13,** 1011 (1992).
28. Hess, B., Kutzner, C., van der Spoel, D. & Lindahl, E. GROMACS 4: algorithms for highly efficient, load-balanced, and scalable molecular simulation. *J. Chem. Theory Comput.* **4,** 435 (2008).
29. Nosé, S. A molecular-dynamics methods for simulations in the canonical ensemble. *Mol. Phys.* **52,** 255 (1984).
30. Hoover, W. G. Canonical dynamics: equilibrium phase-space distributions. *Phys. Rev. A* **31,** 1695 (1985).
31. Parrinello, M. & Rahman, A. Polymorphic transitions in single crystals: a new molecular dynamics method. *J. Appl. Phys.* **52,** 7182 (1981).
32. Essmann, U. *et al.* A smooth particle mesh Ewald method. *J. Chem. Phys.* **103,** 8577 (1995).
33. Harms, S. *et al.* Free volume of interphases in model nanocomposites studied by positron annihilation lifetime spectroscopy. *Macromolecules* **43,** 10505 (2010).
34. Jacquemin, J., Costa Gomes, M. F., Husson, P. & Majer, V. Solubility of carbon dioxide, ethane, methane, oxygen, nitrogen, hydrogen, argon, and carbon monoxide in 1-butyl-3-methylimidazolium tetrafluoroborate between temperatures 283 K and 343 K and at pressures close to atmospheric. *J. Chem. Thermodyn.* **38,** 490 (2006).